# USAAVLABS Tandem Rotor Airloads Measurement Program

R. R. PRUYN*
*The Boeing Company, Morton, Pa.*

AND

W. T. ALEXANDER JR.†
*U. S. Army Aviation Materiel Laboratories, Fort Eustis, Va.*

**An Army CH-47A helicopter has been extensively instrumented and flight-tested to measure the steady and dynamic loads on the rotors, controls, and airframe. The test conditions included high blade loadings and a range of flight speeds from hovering through transition and up to the rotor stall-limited speed. Measurements of a comprehensive array of blade airload pressures and the resulting blade bending, rotor hub motions, rotor shaft loads, control loads, and fuselage response have been obtained. Automatic analog-to-digital data processing techniques were utilized. Initial results of this program are presented which show significant airload pressure variations due to rotor tip vortex interference. Blade section pressures can differ considerably from those of a two-dimensional airfoil over significant areas of the rotor disk, apparently due to the combined effects of compressibility and the disturbances from tip vortex interference. Integrated airload pressure data show that the azimuthal average loading on the forward rotor of a tandem is nearly constant with radius, apparently due to the upwash caused by the aft rotor. A suggested approach to reducing rotor blade airloads data to synthesized airfoil section data is presented.**

## Nomenclature

$a_f$, $a_r$ = angle of inclination of rotor shaft of forward and aft rotors, respectively (used for comparative wind-tunnel data only), positive when inclined downwind, deg
$C_{MP}(0.25c)$ = pitching moment coefficient, calculated from pressure measurements using theoretical local resultant velocity, moment referred to the 25% chord
$C_{NP}$ = normal force coefficient, calculated from pressure measurements using theoretical local resultant velocity
$C_{TW/\sigma}$ = average thrust-coefficient/solidity ratio (based on run gross weight)
$|l_3|$ = third harmonic airload ratio, third harmonic resultant of lift per unit span divided by the run gross weight per unit of total blade length
$M(1.0, 90)$ = Mach number of the tip of the advancing rotor blade at 90° azimuth
$M(0.95, 90)$ = Mach number at 95% radius and 90° azimuth
$r$ = spanwise distance from the center of rotation to a particular blade station, in.
$R$ = rotor tip radius, in.
$\mu'$ = rotor advance ratio, calibrated true airspeed of the helicopter divided by the rotational tip speed of the rotor
$\psi$ = rotor azimuth angle, measured from downwind position in direction of rotation, deg

## Introduction

THE U.S. Army Aviation Laboratories (USAAVLABS) dynamic airloads measurement research efforts have included in-flight measurements on various contemporary helicopter configurations. The presently reported effort is the most ambitious of these efforts with simultaneous measurements of airloads, blade dynamics, control loads, and airframe response being made on both rotors of a tandem configuration. This effort is related to the previous dynamic airloads tests as shown in Table 1. Analytical programs to make use of these data[13,14] have also been supported by USAAVLABS. These programs have stimulated rotor research and have contributed to a fund of knowledge that the industry is now trying to utilize to improve helicopter efficiency.

## Rotor Wake Effects

Previous rotor airloads measurement programs have shown that rotor wakes are dominated by the rather large

**Table 1 Relationships between present tests and existing rotor airloads data**

| | | ROTOR GEOMETRY | | | | |
|---|---|---|---|---|---|---|
| | | SINGLE ROTOR | | | TANDEM ROTOR | |
| BLADES PER ROTOR | | 2 | 3 | 4 | 2 | 3 |
| SMALL MODELS (ROTOR DIAMETER < 8 FEET) | | | | | | |
| HUB CONFIGURATION | TEETERING | - | - | - | - | - |
| | FULLY ARTICULATED | Meyer and Falabella (1) | - | - | - | - |
| LARGE MODELS (ROTOR DIAMETER ≥8 FEET) | | | | | | |
| HUB CONFIGURATION | TEETERING | Rabbott (2,3) Mayo(4) | - | - | Huston (5) | - |
| | FULLY ARTICULATED | - | Ham (6) | X | - | Ham (7) |
| FULL SCALE (WIND TUNNEL OR FLIGHT TEST) | | | | | | |
| HUB CONFIGURATION | TEETERING | Burpo (8,9) | X | - | - | - |
| | FULLY ARTICULATED | - | X | Scheiman (10) Rabbott (11) | - | Present Tests Gabel (12) |

Presented as Paper 66-735 at the AIAA Aerodynamic Testing Conference, Los Angeles, Calif., September 21–23, 1966; submitted September 28, 1967; revision received February 15, 1967. The work described herein has been sponsored by the U. S. Army under Contract DA 44-177-AMC-124(T). [6.01]

* Supervisory Engineer for Advanced Rotor Structures, Vertol Division. Associate Member AIAA.

† Head of Dynamics (Acting), Aeromechanics Division.

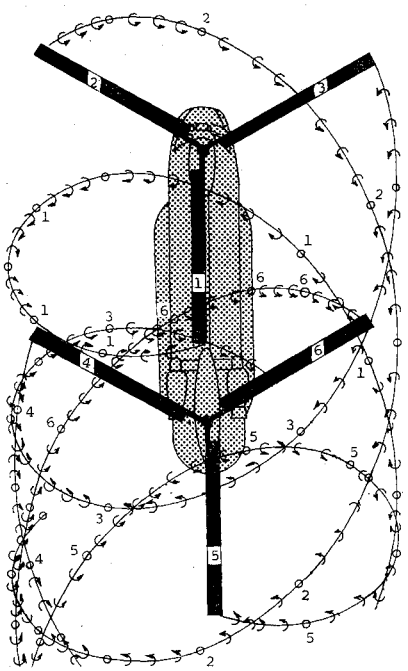

**Fig. 1 Blade tip vortex trajectories of a tandem rotor helicopter.**

disturbances caused by the blade tip vortexes. If it is assumed that the wake is rigid and the advance ratio is about 0.5, the rotor blade tip vortex trajectories of a tandem helicopter are as shown in Fig. 1. For convenience of description, the blades and their respective tip vortexes are identified by numbers in this figure. Since these vortexes decay with time, only those vortexes formed on the rotor revolution being considered are significant. It should be further noted that this wake is unstable and is not rigid, so that nearby vortexes of the same sign (rotation direction) will revolve about one another. Adjacent vortexes of similar strength but opposite sign will cause each other to translate.

The proximity of the tip vortexes to the blade is reflected by large local pressure oscillations in the blade airload pressures. These pressure oscillations are generally of relatively little consequence in the integrated airloads. On the advancing blade, where the local Mach number can approach unity, the tip vortex proximity apparently triggers a significant and persisting change in the chordwise pressure distribution; therefore, those tip vortexes which influence the advancing blade should be especially noted.

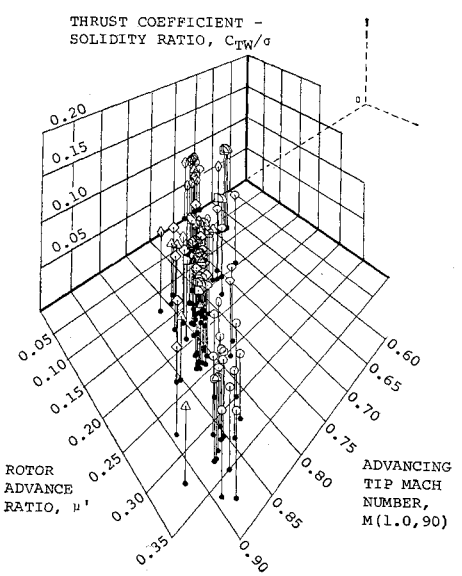


**Fig. 2 Some rotor aerodynamic parameters of the conditions tested.**

An additional consideration that should be noted in the discussion of the rotor wake is the angle between the vortex and the blade. If this angle is small, the effect of the vortex will be large. Fortunately, most of the vortex crossings occur with large intersection angles, so that the effects of the vortex are less severe and are spread over a larger portion of the azimuth.

It can be seen in Fig. 1 that as the forward blades cross the fuselage, the blade outer ends are near a vortex trailed by the aft blades (e.g., blade 6 in the figure). The intersection angle of blade 1 and vortex 6 is generally large. As it continues around the azimuth, blade 1 then intersects its own tip vortex with a small intersection angle. Blade 1 will then come into close proximity with the vortexes from blades 2 and 3 as it continues through the advancing half of the revolution; these intersections are at large angles. On the retreating half of the revolution, the blades encounter the tip vortex from the preceding blade; this proximity is usually detectable since the intersection angle is small.

For the aft rotor there are many more vortexes to consider, but there is only one additional crossing which is at a small intersection angle. That is the intersection of blade 4 with vortex 1 near 120° azimuth of the aft rotor. This intersection can be particularly severe since the vortex has not had time to decay and the intersecting aft blade is moving at relatively high speed. Fortunately, longitudinal cyclic trim is available on the tandem helicopter to adjust the relative inclinations of the two rotors, so that this aft rotor blade vortex intersection can be avoided.

A further peculiarity of the tandem configuration which should be considered in the discussion of the rotor wake is the average rotor-rotor interference. It has been known for some time that the forward rotor causes an increase in the downwash at the aft rotor. This downwash causes the tip vortexes to move rapidly away from the plane of the rotor. Thus the vortexes shown in Fig. 1, which were formed earlier in the rotor revolution, do not have a significant influence on the aft rotor. An unexpected finding of this tandem rotor airloads program is that the aft rotor causes an upwash at the forward rotor. This upwash is reflected in the average rotor loading and, in retrospect, should have been anticipated from the available rotor-induced flow measurements and theories. The significance of this upwash on the rotor wake is that the forward rotor vortexes do not move away from the rotor as anticipated, so that relatively old vortexes remain sufficiently close to the rotor to cause disturbances in the blade pressures.

## Test Program Formulation

The test program to measure dynamic airloads consisted of a matrix of rotor speeds, helicopter airspeeds, gross weights, and altitudes to fully explore the available range of thrust coefficient, advance ratio, and advancing tip Mach number capability of the test helicopter. The achieved test conditions of the level flight portion of the flight program are shown in nondimensional form in Fig. 2. It should be noted that a wide range of data has been obtained. Accomplished test conditions have included advancing tip Mach numbers greater than 0.9 and advance ratios approaching 0.40. During all these tests, a thrust coefficient solidity ratio greater than 0.060 was obtained.

## Airframe and Instrumentation Characteristics

The geometry of the test helicopter is presented in Fig. 3. In external configuration this helicopter was a standard CH-47A, but through years of experimental flight testing, numerous detail changes had been incorporated. The instrumentation utilized in this test program and the basic data reduction

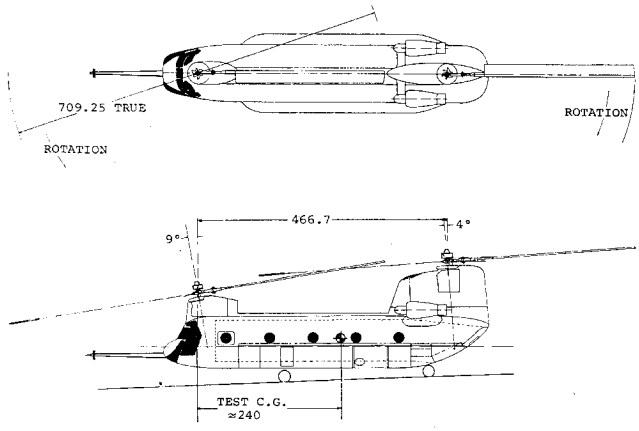


**Fig. 3 General arrangement of CH-47A helicopter as tested.**

methods are detailed elsewhere,[16] so that ony a brief review of these aspects of the program is included in this paper.

Principal interest was directed to the blade system with the extensive pressure instrumentation illustrated in Fig. 4 as the primary means of measurement. Supporting these measurements were blade bending strain gages and blade hinge angle transducers. Since the airloads bend the blades, measuring both bending and airloads is somewhat redundant, but there was interest in the magnitude of the contribution of blade elastic effect and in the blade structural response. The blade loads were also measured as rotor shaft loads and control system loads. Rotor hub, rotor shaft, and fuselage motions due to the rotor loads were also measured. An array of fuselage vibration accelerometers was also utilized. By providing instrumentation at each interface of the dynamic system, similar measurements can be related to give more information than can be obtained from the same number of separate measurements. These data are accurate to at least the tenth harmonic.

## Rotor Airloads Measurements

Rotor blade differential pressures (upper surface pressure minus lower surface pressure) near the leading edge of the blade are very sensitive to detailed variations in the local flow; these data are therefore informative separately as well as in relation to the other pressures along the chord. Following chordwise integration these data become less sensitive to detailed variations but are more useful in indicating rotor performance and vibratory excitations. Blade section aerodynamic performance is more clearly indicated when the chordwise integrated airloads data are reduced to coefficient form. Illustrations of airloads data in each of these various forms are presented.

### Airloads Pressure Data

Figure 5 shows azimuthal variations in the local differential pressures at three chordwise locations at 85% radius on the forward and aft rotors. This figure contains all the data measured during 5 separate rotor cycles. The envelopes of data shown are within 5% of the mean for any azimuth. This repeatability between rotor cycles is better than expected since wake instability and flight path variations were thought to be more significant.

A comparison of the data for the three chordwise locations of Fig. 5 shows a greater sensitivity to the effects of vortex proximity at the 13% chord. This is believed to be due to compressibility effects at the large angles of attack involved, which reduce the leading-edge pressures and amplify the pressures near the quarter-chord. Blade sections are characteristically relatively fragile aft of the quarter-chord due to

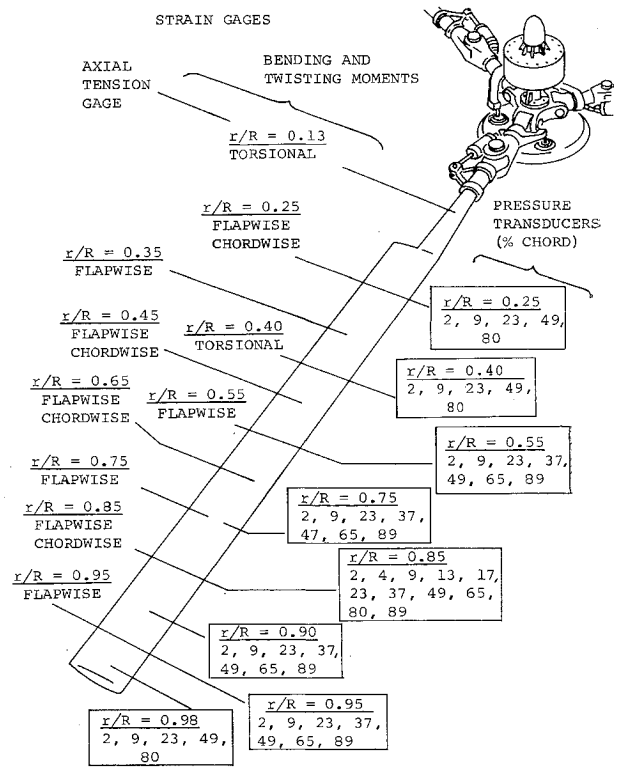


**Fig. 4 Rotor blade instrumentation.**

blade balancing requirements, so that the small alternating loads in this region are fortuitous.

A comparison of the forward and aft rotor data of Fig. 5 shows that the forward rotor pressures reflect many vortex proximity situations but that the aft rotor pressures are dominated by a large 2-cycle disturbance. The forward rotor data show a pronounced oscillation as the blade crosses its own tip vortex at about 40° azimuth. As the forward blade continues around the azimuth, it experiences oscillations centered at 160° and 270°. The first of these oscillations is of a down-up sign since the vortex of the following blade was crossed from the inside. The second oscillation is of opposite polarity since it is apparently due to crossing the tip vortex of the preceding blade from the outside. The latter oscillation is also apparent in the aft rotor data.

The dominant oscillation of the aft rotor pressures cannot be explained in detail, but it is reasonably certain that the large second cycle of this oscillation is due to the up-down disturbance of the tip vortex from the preceding blade of the

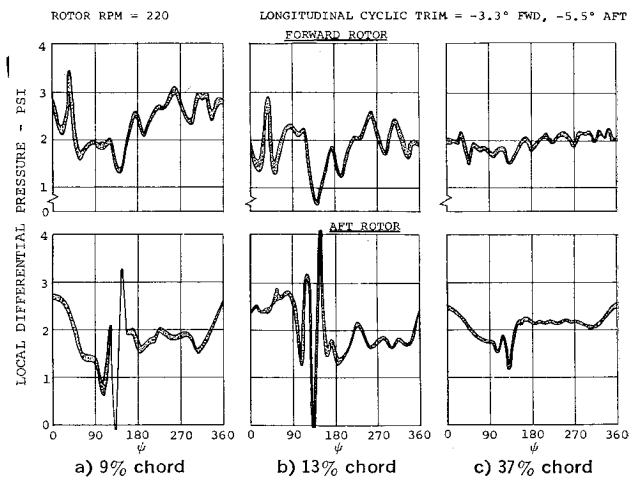


**Fig. 5 Azimuthal variation of typical pressure measurements (85% radius) at 108 knots and 26,000-lb gross weight.**

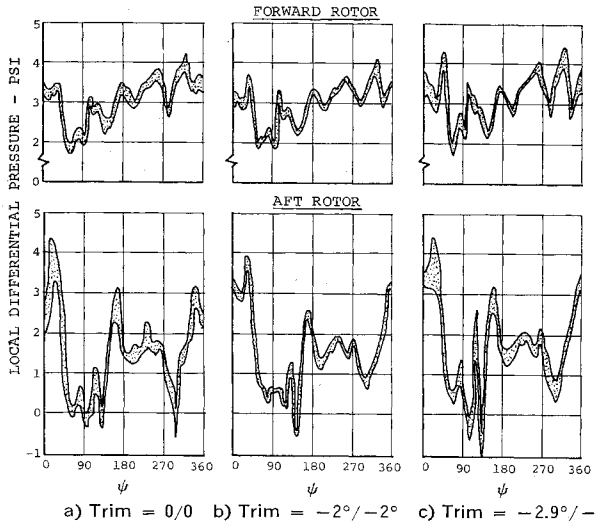


**Fig. 6 Effect of trim setting on rotor airload pressures (85% radius, 9% chord) at 100 knots and 33,000-lb gross weight.**

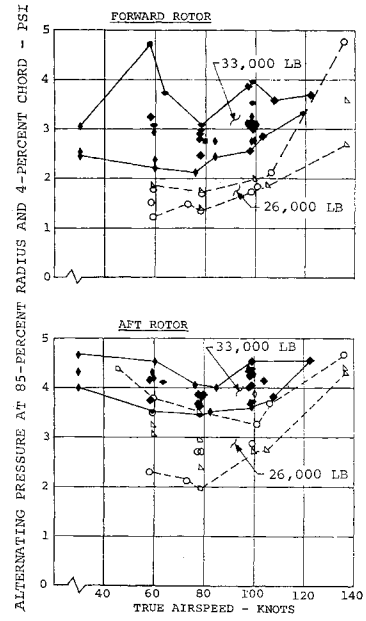


**Fig. 8 Alternating local blade pressures for a summary of level flight conditions.**

forward rotor. The first part of this oscillation is apparently due to the down-up disturbance of the following blade of the aft rotor. Between these two identifiable disturbances there is an unaccounted-for half-cycle of the oscillation.

The local blade pressures contain somewhat larger oscillations at heavier gross weights, and the aft rotor data are significantly changed by longitudinal cyclic trim, as shown in Fig. 6. It should first be noted that the data for this figure were obtained at a slightly higher rotational speed. This increase, together with the larger blade section angle of attack required for the increased weight, resulted in a significant increase in compressibility effects. Figure 6 shows this by the rather sudden decrease in pressure near 40° azimuth with the pressure remaining low until about 110° on the forward rotor. The aft rotor pressure does not recover until after the large forward rotor vortex interference oscillation.

Since it changes the relative orientation of the two rotors, cyclic trim has a large effect on the tip vortex interference oscillations of the aft rotor pressures. As shown in Fig. 6, these oscillations are much larger with extended trim (−2.9°/−4.7°) than they are with zero trim. This trend of increased interference with increased trim is generally applicable to all gross weights and speeds, since increased trim moves the aft rotor down into the wake of the forward rotor. Extended trim is beneficial for other reasons, so that a trim optimization is required. The only problem known to be caused by vortex interference is increased rotor noise.

A typical response of the chordwise pressure distribution to the vortex interference spike of the aft blade is shown in Fig. 7. A saw-tooth pattern between 2 and 23% of the chord is shown with the amplitude of the variations increasing

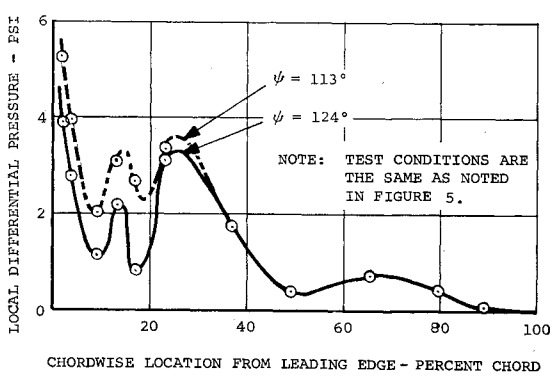


**Fig. 7 Typical chordwise pressure distributions of aft rotor in proximity of forward rotor tip vortex.**

as the azimuth angle increases from 113° to 124°. It requires about 50° of azimuth travel before the blade section performance returns to a two-dimensional character. It appears that the response of the pressure distribution is influenced significantly by compressibility effects that are three-dimensional. These effects cause the response to persist and to couple the responses of adjacent blade sections.

It was suspected that the data presented which show the large airload oscillation spikes are not typical. In support of this suspicion is the pronounced effect of longitudinal cyclic pitch trim setting on rotor noise. To evaluate the frequency of occurrence of spiking interferences, a stress-oriented computer program was utilized to sort the airloads data and to determine the values of half of the difference between the

| SYMBOL | TRUE AIRSPEED KNOTS | LONGITUDINAL CYCLIC TRIM FWD/AFT | RUN NUMBER | TEST POINT NUMBER |
|---|---|---|---|---|
| ◇ | 54 | -1.1/-0.9 | 3 | 61 |
| ● | 98 | -3.3/-5.2 | 4 | 18 |
| ◇ | 138 | -3.9/-5.4 | 5 | 36 |

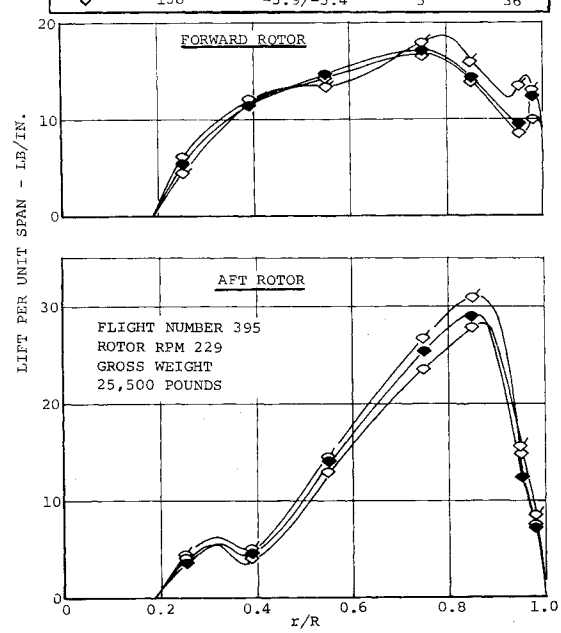


**Fig. 9 Azimuthal average loading of the tandem rotors showing pronounced interference effects.**

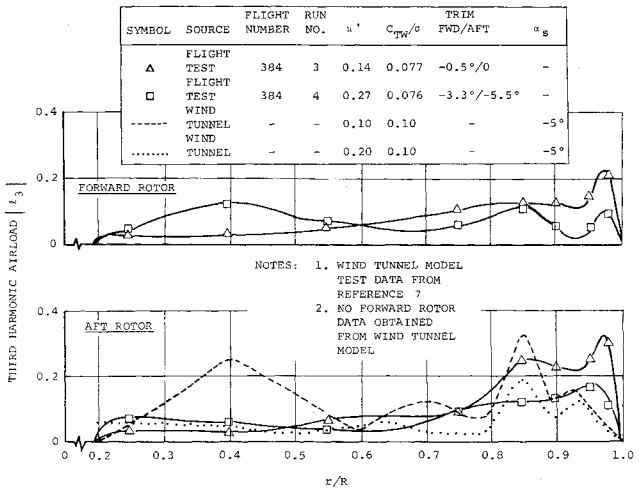


**Fig. 10 Third harmonic airloads from flight-test data with comparative tandem rotor model data.**

maximum and the minimum pressures which occurred in any one of the measured rotor cycles. This value was defined as the alternating airload pressure. The alternating values of airload pressure at the 85% span and 4% chord position for all flight conditions are shown in Fig. 8. A pronounced effect of gross weight between the 26,000- and 33,000-lb gross weight test points is shown, with considerable variation between the various 33,000-lb test points. Testing at 33,000 lb included considerable variation in the cyclic trim, and, as shown previously, the trim setting does produce a sizable shift in the vortex interference effects. However, the general consistency of the data of Fig. 8 indicates that large pressure oscillations occur for most flight conditions.

### Integrated Airload Pressure Data

The chordwise integrated steady airloads, that is, the azimuthal average lift per unit span for three flight conditions, are shown in Fig. 9. It can be seen that the forward rotor loading is fairly uniform and that the airload distribution of the aft rotor is similar to that of a hovering rotor. The aft rotor data show an unexpected large relief of the average lift near the tip, possibly due to vortex interference effects. Airspeed does not appear to have much effect on these data. The differences in the average loadings of the two rotors are attributed to an upwash at the forward rotor caused by the

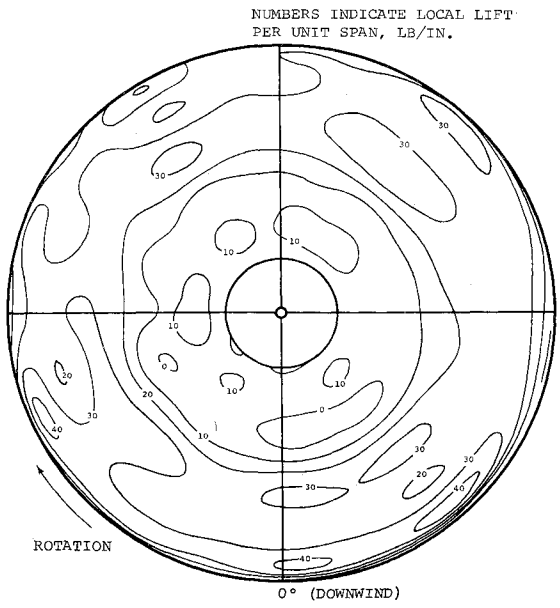


**Fig. 11 Contour plot of lift per unit span of aft rotor at 108 knots and 26,000-lb gross weight.**

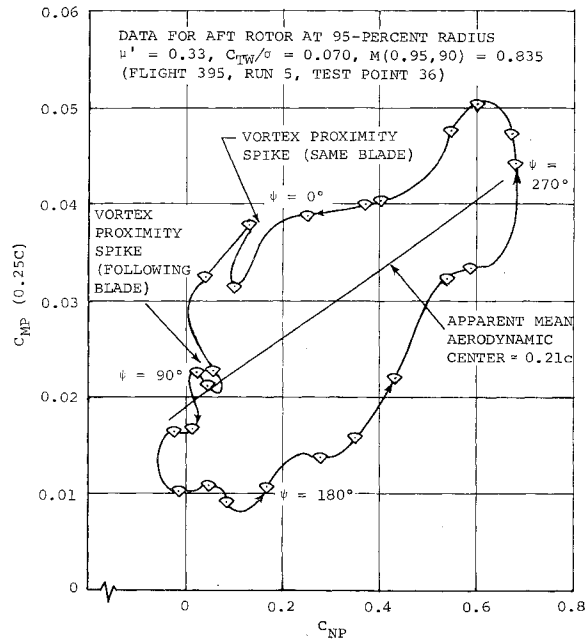


**Fig. 12 Aerodynamic pitch moment damping of a test point with no effects of stall or compressibility.**

aft rotor. This upwash produces larger inboard loadings on the forward rotor blades than those of an equivalent isolated rotor.

The third harmonic components of the airloads data for two similar flight conditions are shown in Fig. 10, where they are compared with wind-tunnel model data.[7] These data show that a sizable portion of the third harmonic airloads are concentrated near the outer ends of the blades, particularly on the aft rotor. This tendency is typical and is believed to indicate that the use of tapered planform blade outer panels may transmit less of these vibratory loads to the helicopter. Fairly good correlation is shown between the wind-tunnel and the flight-test data with similar magnitudes obtained, but the distribution of the loading is somewhat different. This difference may be due to the more rigid blades of the model.

A contour plot of these airload lift per unit span data for the aft rotor at 108 knots is shown in Fig. 11. These data are reasonably smooth except for small regions of high load at 65°, 150°, 220°, 320°, and 350° azimuth. There does not appear to be a significant correlation between these high load regions and the tip vortex pattern. The concentration of the largest oscillating airloads on the outer portion of the blade is also shown by this figure.

## Analysis of Rotor Airloads Data

The Tandem Rotor Airloads Measurement Program has produced a significant addition to the large volume of rotor airloads data which has been available since 1962. It is generally acknowledged in the helicopter industry that the acquisition of these data is worth the time and expense required, but at the present time the industry appears to have made only limited use of these data. While the objective of this paper is to provide an introduction to this project, some comment as to the reasons for this apparent contradiction and a recommended approach to resolve the situation are believed to be warranted.

The most significant use of the existing airloads measurements has been for the development of nonuniform downwash rotor theories. This development has received considerable benefit from correlations[13–15] with the airloads measurements, and it is expected that this utilization will continue. However, the value of this form of utilization will diminish steadily since nonuniform downwash theory is presently of acceptable accuracy and is used in a fairly routine manner.

The rotor airloads data have been shown[17] to contain information on the dynamic response of blade section aerodynamic performance, blade section stall, compressibility, and the effects of local section sweep angle variations. This effort substantiated a previous study[18] of rotor airloads data which showed that blade stall was indicated by the blade section pitching moments calculated from the airload pressures. These efforts are believed to be the start of the evolution of an aerodynamic blade stall criterion and the start of the evaluation of airfoil characteristics from the airloads measurements. These tasks are difficult because of the following peculiarities of rotor airloads data: 1) The data required to describe a test point adequately are voluminous and complex. 2) Blade section pitching moment data are sensitive to small pressure measurement errors. 3) Compressibility, vortex proximity, etc., cause irregularities in the data which are difficult to analyze. 4) Airloads data tend to be inconsistent due to wake instabilities, atmospheric disturbances, and helicopter motions.

A key to the understanding of these data, achieved at the penalty of an additional complication in data handling, is the presentation of the airloads data in the form shown in Fig. 12. This illustration provides an indication of the aerodynamic pitch moment damping, which has a sizable influence on rotor blade loads. The indication of damping from the $C_{NP}$-$C_{MP}$ relation depends on the linear relationship of $C_{NP}$ and the local instantaneous angle of attack. Since the dynamic-aerodynamic environment appears to prevent lift-stall, and potential flow theory indicates that there is little phase shift in the lift-to-angle-of-attack relation, the assumption of a linear $C_{NP}$-to-angle-of-attack relationship is justified. As shown in Fig. 12, the $C_{NP}$-$C_{MP}$ relation has the advantage of showing the integrated significance of the vortex proximity spikes. For more severe conditions, stall and compressibility effects are shown as a breakdown of the generally elliptical $C_{NP}$-$C_{MP}$ relation and indicate a region of negative aerodynamic damping.

It is anticipated that the greatest benefit to be obtained from the airloads measurements will come from attempts to resolve these data into synthesized airfoil data. This synthesis follows previous efforts[19] to generate airfoil data that utilized hovering rotor performance data; however, the use of airloads measurements is far more straightforward. A theoretical angle of attack, based on either a nonuniform downwash rotor analysis or an evaluation of the angle of attack from the normal force data, can be used as a basis for the airfoil data. The effects of the first and higher harmonic variations in angle of attack and the effects of blade section sweep should be considered in this analysis as well as the more obvious compressibility and blade stall considerations.

## Conclusions

1) Consistent measurements of the dynamic airloads of a tandem rotor helicopter have been obtained using instrumentation with adequate resolution and response to record all significant rotor wake and blade dynamic effects.

2) Adversely trimmed flight configurations can cause sharp wake vortex interference spikes in the rotor airload pressure measurements.

3) Rotor tip vortex interference is indicated by a large, suddenly applied change in local blade section pressures. The largest magnitude of this change tends to occur near the quarter-chord of the blade section. Vortex interference causes a saw-toothed shape in the chordwise pressure distribution, due apparently to compressibility effects.

4) The azimuthal average loading on the forward and aft rotors of a tandem helicopter is significantly different. Average forward rotor loading is more uniform with radius than an isolated rotor, apparently because of an upwash from the aft rotor.

5) Oscillating airloads tend to be concentrated toward the tips of the blades.

6) A combined experimental-analytical method of isolating rotor airfoil performance from dynamic airloads measurements has been devised and is being utilized to interpret these measurements.

## References

[1] Meyer, J. R. and Falabella, G., "An investigation of the experimental aerodynamic loading on a model helicopter rotor blade," NACA TN 2953 (1953).

[2] Rabbott, J. P., "Static-thrust measurements of the aerodynamic loading on a helicopter rotor blade," NACA TN 3688 (July 1956).

[3] Rabbott, J. P. and Churchill, G. B., "Experimental investigation of the aerodynamic loading on a helicopter blade in forward flight," NACA RM L56107 (October 1956).

[4] Mayo, A. P., "Comparison of measured flapwise structural bending moments on a teetering rotor blade with results calculated from the measured pressure distribution," NASA Memo 2-28-59L (March 1959).

[5] Huston, R. J., "Wind tunnel measurements of performance, blade motions, and blade airloads for tandem rotor configuration with and without overlap," NASA TN D-1971 (October 1963).

[6] Ham, N. D., "An experimental investigation of the effect of a nonrigid wake on rotor blade airloads in transition flight," Cornell Aeronautical Laboratory/TRECOM Symposium on Dynamic Load Problems Associated with Helicopters and V/STOL Aircraft, Proceedings, Vol. I (June 1963).

[7] Ham, N. D. and Madden, P. A., "An experimental investigation of rotor harmonic airloads including the effects of rotor-rotor interference and blade flexibility," U.S. Army Transportation Research Command, Rept. TCREC TR 65-13 (May 1965).

[8] Burpo, F. B., "Measurement of dynamic airloads on a full-scale semirigid rotor," Transport Research and Engineering Command Rept. 62-42 (December 1962).

[9] Burpo, F. B., "Summary report—Development of a subminiature surface mounted pressure transducer," Bell Helicopter Co., Rept. 299-099-200, Contract NOnr 2877(00) (January 1963).

[10] Scheiman, J., "A tabulation of helicopter rotor blade differential pressures, stresses, and motions as measured in flight," NASA TM X952 (March 1964).

[11] Rabbott, J. P., Lizak, A. A., and Paglino, V. M., "A presentation of measured and calculated full scale rotor blade aerodynamic and structural loads," U. S. Army Aviation Labs. TR 66-31 (1966).

[12] Gabel, R., et al., "AVID Program, advanced vibration development," Boeing-Vertol Rept. 107M-D-09, Contract NOw-62-0177f (April 1965).

[13] Piziali, R. A. and DuWaldt, F. A., "A method for computing rotary wing airload distributions in forward flight," Transport Research and Engineering Command, Rept. TCREC TR 62-44 (November 1962).

[14] Segel, L., "A method for predicting the nonperiodic airloads on a rotary wing," AIAA Paper 66-17 (1966); also J. Aircraft **3**, 541–548 (1966).

[15] Davenport, F. J., "A method for computation of the induced velocity field of a rotor in forward flight, suitable for application to tandem rotor configurations," J. Am. Helicopter Soc. 9 (July 1964).

[16] Pruyn, R. R., Obbard, J., and Shakespeare, C., "The measurement and analysis of rotor blade airloads and the resulting dynamic response of a large tandem rotor helicopter," Instrument Society of America, The Fourth International Instrumentation Symposium, Cranfield, England (March 1966).

[17] Pruyn, R. R., et al., "In-flight measurement of rotor blade airloads, bending moments, and motions, together with rotor shaft loads and fuselage vibration, on a tandem rotor helicopter," Boeing Doc. D8-0382, U. S. Army Aviation Labs. TR 67-9, to be published).

[18] Scheiman, J. and Kelley, H. L., "Comparison of flight-measured helicopter rotor blade chordwise pressure distributions and two-dimensional airfoil characteristics," Cornell Aeronautical Laboratory/TRECOM Symposium on Dynamic Load Problems Associated with Helicopters and V/STOL Aircraft, Proceedings, Vol. I (June 1963).

[19] Carpenter, P. J. and Shivers, J., "Effects of compressibility on rotor hovering performance and synthesized blade-section characteristics derived from measured rotor performance of blades having NACA 0015 airfoil tip sections," NACA TN 4356 (September 1958).